Supplement Section S.1

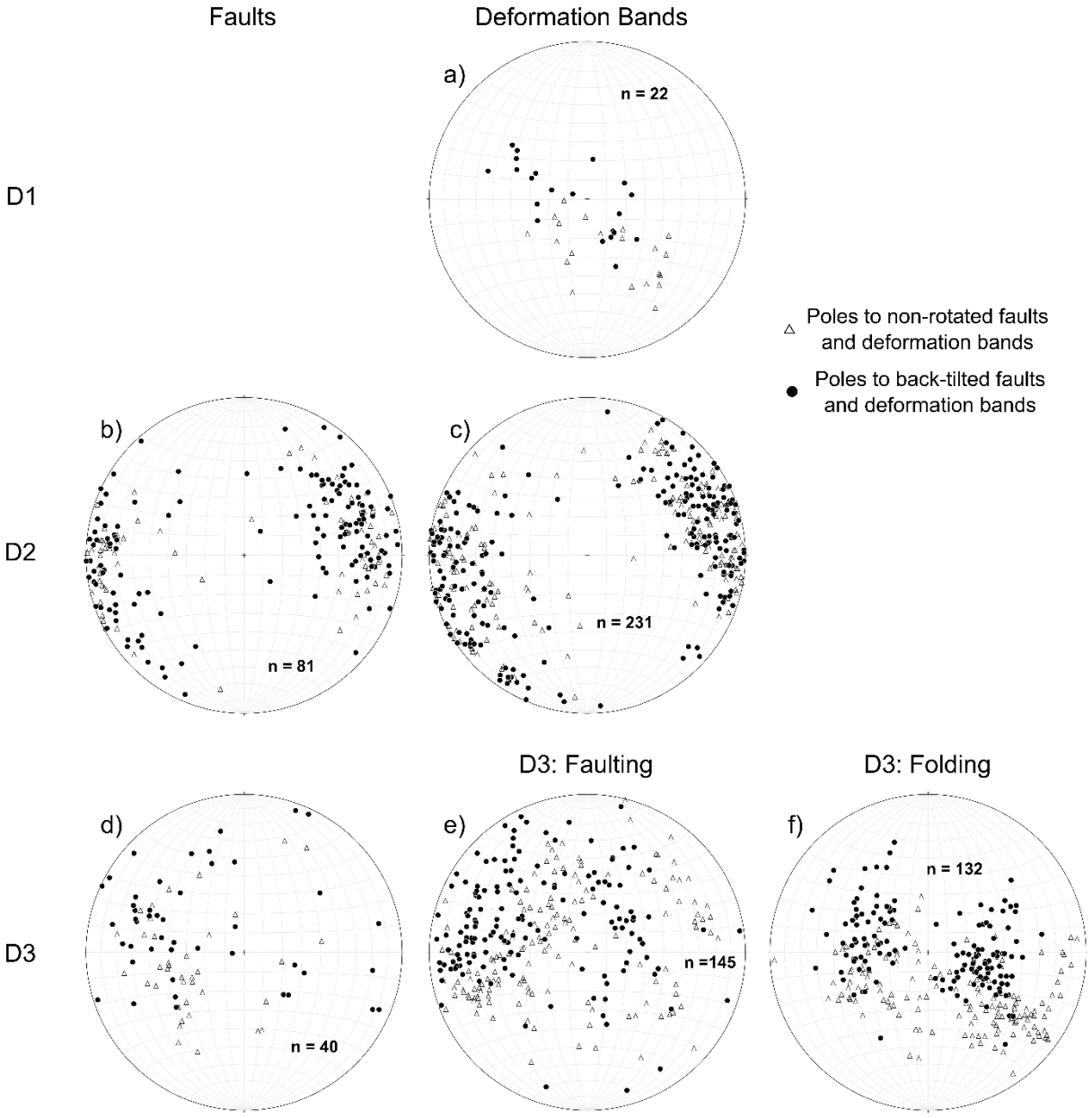

Figure S1.1. Schmidt nets of back-tilted orientations of structural features compared with present-day orientations. Structural data was back-tilted using the nearest S_0 measurement in Stereonet 10 (Allmendinger et al., 2011). a) Deformation bands associated with D1 faulting. b) Normal faults formed during D2 horizontal extension. c) Deformation bands with normal-sense shear formed during D2 horizontal extension. d) Reverse faults formed during D3 horizontal contraction. e) Deformation bands with reverse-sense shear formed during D3 horizontal contraction. f) Deformation bands with a regular spacing and minimal offset observed in areas of folded sandstone beds, formed during D3 horizontal contraction. Tight clustering of these bands when in their original orientation indicates that they have since been rotated with folding.

Supplement Section S.2

Table S2.1. Table of microfabric data for analysed thin sections.

	Sample	Band width (mm)	Host rock average perimeter (um)	DB average perimeter (um)	HR diameter (um)	DB Diameter (um)	Aspect ratio (HR)	Aspect ratio (DB	Grainsize Reduction (%)	Band offset (mm)	DB porosity	DB porosity fraction	HR Porosity	HR porosity fraction	Weights	DB neg error	DB pos error	HR neg error	HR pos error	Dc	Dc/Dc	Dihedral angle	Porosity Reduction	Matrix spacing (um)	Damage zone Width (cm)	Fault offset (km)	Band thickness (mm)	Location (lat)	Location (long)	Type of Band	Lithology (Facies)
D2 FDZ	48.1	0.636	171.65	59.39	54.64	18.90	1.63	1.68	35%	4.40	7.30	0.07	13.50	0.13	0.19	1.33	1.36	2.10	2.13	0.05	96.59	N/A	6.20	NL	12.00	30.00	N/A	-40.938763	176.169680	Normal CSB	FA3
	97.4	1.505	257.44	147.21	81.95	46.86	1.50	1.63	57%	6.20	4.93	0.05	12.66	0.13	0.23	1.13	1.13	1.62	1.64	0.13	46.56	N/A	7.73	NL	> 55 cm IDZ	195.00	N/A	-40.925111	176.190607	Normal CSB	FA2
	97.1.2	1.300	195.57	157.03	62.25	49.98	1.58	1.61	80%	8.30	2.89	0.03	9.83	0.10	0.22	0.64	0.63	1.53	1.54	0.10	82.96	N/A	6.94	NL	> 55 cm IDZ	195.00	N/A	-40.925111	176.190607	Normal CSB	FA2
	131.5	0.877	283.55	161.85	90.26	51.52	1.55	1.58	57%	5.60	8.49	0.08	17.43	0.17	0.22	1.82	1.84	2.49	2.55	0.09	59.01	N/A	8.94	NL	> 30 cm IDZ	55.00	N/A	-40.929451	176.181770	Normal CSB	FA2
	74.3	0.917	216.14	65.17	68.80	20.75	1.62	1.60	30%	6.10	7.96	0.08	18.71	0.19	0.15	1.15	1.16	1.61	1.64	0.12	50.31	N/A	10.74	NL	4.00	31.00	N/A	-40.936817	176.173234	Normal CSB	FA2
	53.3.2	0.939	213.39	56.61	67.92	18.02	1.76	1.14	27%	5.50	8.08	0.08	17.17	0.17	0.22	1.76	1.77	2.19	2.24	0.10	53.33	N/A	9.09	NL	> 200 cm IDZ	> 10 m	N/A	-40.938075	176.170602	Normal CSB	FA3
	53.1.2	0.807	143.51	86.23	45.68	27.45	1.65	1.58	60%	4.80	7.04	0.07	13.19	0.13	0.17	1.18	1.18	2.06	2.08	0.06	83.95	N/A	6.15	NL	> 200 cm IDZ	> 10 m	N/A	-40.938075	176.170602	Normal CSB	FA3
	53.1.1	0.952	258.45	61.45	82.27	19.56	1.58	1.63	24%	6.10	5.55	0.06	14.12	0.14	0.22	1.22	1.21	2.27	2.29	0.10	64.19	N/A	8.57	NL	> 200 cm IDZ	> 10 m	N/A	-40.938075	176.170602	Normal CSB	FA3
	53.3.1	0.742	245.68	74.61	78.20	23.75	1.67	1.65	30%	6.20	8.93	0.09	16.71	0.17	0.12	0.99	1.03	1.96	1.89	0.07	89.48	N/A	7.78	NL	> 200 cm IDZ	> 10 m	N/A	-40.938075	176.170602	Normal CSB	FA3
	101.1	0.827	254.32	115.02	80.95	36.61	1.62	1.69	45%	3.20	6.04	0.06	19.09	0.19	0.19	1.16	1.14	2.60	2.64	0.13	23.99	N/A	13.05	NL	0.10	4.00	N/A	-40.944526	176.160817	Normal CSB	FA3
D3 FDZ	141.1.2	1.830	217.33	84.30	69.18	26.83	1.71	1.66	39%	11.20	12.03	0.12	26.09	0.26	0.25	2.99	3.01	2.62	2.72	0.35	32.16	N/A	14.06	NL	145.00	3.00	N/A	-40.941299	176.165649	Reverse CSB	FA3
	74.5	0.639	178.99	44.62	56.97	14.20	1.53	1.68	25%	6.80	13.30	0.13	21.19	0.21	0.19	2.52	2.55	2.00	2.04	0.06	106.30	N/A	7.89	NL	6.00	12.00	N/A	-40.936817	176.173234	Reverse CSB	FA2
	96.1	0.791	246.35	147.98	78.41	47.10	1.61	1.57	60%	3.80	12.53	0.13	19.20	0.19	0.17	2.07	2.10	2.19	2.24	0.07	58.18	N/A	6.67	NL	272.00	10.00	N/A	-40.930442	176.180182	Reverse CSB	FA2
	141.1	1.979	209.30	93.24	66.62	29.68	1.67	1.64	45%	5.60	11.15	0.11	16.57	0.17	0.22	2.45	2.47	2.16	2.21	0.13	43.52	N/A	5.42	NL	145.00	3.00	N/A	-40.941299	176.165649	Reverse CSB	FA3
	141.1.1	1.513	202.43	76.17	64.44	24.24	1.57	1.53	38%	6.20	13.48	0.13	18.08	0.18	0.18	2.37	2.42	1.82	1.87	0.09	72.92	N/A	4.60	NL	145.00	3.00	N/A	-40.941299	176.165649	Reverse CSB	FA3
D3 non-FDZ	1.1	1.002	157.36	92.49	50.09	29.44	1.71	1.69	59%	0.10	11.86	0.12	20.09	0.20	0.16	1.87	1.91	1.49	1.52	0.10	0.97	88.00	8.24	11.80	N/A	N/A	80.10	-40.939025	176.168786	SECB	FA3
	3.1	0.581	173.15	104.68	55.12	33.32	1.68	1.64	60%	0.02	8.63	0.09	16.01	0.16	0.14	1.21	1.22	1.51	1.52	0.05	0.39	76.00	7.38	6.80	N/A	N/A	40.90	-40.938891	176.169167	SECB	FA3
	4.1	0.526	166.19	104.54	52.90	33.28	1.68	1.66	63%	0.08	8.71	0.09	20.01	0.20	0.19	1.63	1.65	1.66	1.70	0.07	1.08	75.00	11.30	2.20	N/A	N/A	29.20	-40.938865	176.169072	SECB	FA3
	11.2	0.695	142.59	98.56	45.39	31.37	1.74	1.65	69%	0.15	6.03	0.06	17.88	0.18	0.16	0.97	0.98	1.31	1.33	0.10	1.50	68.00	11.85	30.00	N/A	N/A	93.80	-40.938841	176.169425	SECB	FA3
	11.3	0.635	76.34	46.40	24.30	14.77	1.76	1.60	61%	0.02	5.16	0.05	17.24	0.17	0.15	0.76	0.77	1.25	1.27	0.09	0.22	68.00	12.08	30.00	N/A	N/A	93.80	-40.938813	176.169415	SECB	FA3

Key		
	FDZ	Fault Damage Zone
	IDZ	Interaction Damage Zone
	CSB	Compactional Shear Band
	SECB	Shear-Enhanced Compaction Band
	FA2	50:50 mudstone to sandstone
	FA3	Sandstone dominated
	HR	Host Rock
	DB	Deformation Band
	NL	Non-Linear

Supplement Section S.3

Table S3.2. Table of results from Pearson correlation coefficient analysis of deformation band spacing.

	Fault	Mean P	Median P	P Range	P IQR
D2 FDZ	Day 23 D2	0.10	0.07	0.62	0.06
	Day 24 D2	0.47	0.60	1.62	0.04
	Fault 14	0.15	0.10	1.19	0.06
	Fault 17.1	0.32	0.33	0.43	0.16
	Fault 17.2	0.62	0.61	0.25	0.04
	Fault 100	0.44	0.46	0.21	0.03
	Fault 161	0.42	0.42	0.62	0.07
D3 FDZ	Day 23 D3	-0.02	0.25	1.36	0.53
	Fault 96	0.13	0.17	1.65	0.10
	Fault 102	0.11	0.22	1.16	0.35
	Fault 117	0.67	0.59	0.43	0.22
	Fault 141	0.66	0.62	0.52	0.05
D3 non-FDZ	Bed 1 Set 2	-0.17	-0.07	0.95	0.04
	Bed 1 Set 1	-0.69	-0.64	0.40	0.09
	Bed 2 Set 2	0.03	-0.10	1.23	0.30
	Bed 3 Set 1	-0.25	-0.27	0.94	0.20
	Bed 4 Set 2	0.09	0.25	1.48	0.59
	Bed 6 Set 1	0.02	0.04	1.11	0.04
	Bed 7 Set 1	-0.15	-0.07	1.17	0.13
	Bed 8 Set 1	0.31	0.32	0.90	0.20
	Bed 9.2 Set 1	0.34	0.34	0.71	0.31
	Bed 10 Set 1	0.42	0.39	0.27	0.17
	Bed 10 Set 1 Main	0.42	0.40	0.32	0.31
	Bed 10 Set 2	0.29	0.31	0.84	0.06
	Bed 11 Set 2	-0.31	-0.32	1.82	0.24
	S1 B1 set 2	-0.39	-0.29	0.81	0.34
	S1 B2 set 1	0.31	0.33	1.50	0.14
	S1 B3 set 1	0.04	0.04	1.49	0.19
	S2 B2 set 1	0.57	0.61	1.68	0.04
	S2 B3 set 1	0.09	0.10	1.21	0.23
	S3 B3 set 2	-0.40	-0.32	0.92	0.60
	Stop 2	-0.73	-0.65	0.63	0.42
	Stop 3	0.37	0.16	1.09	0.90
	Stop 4 bed 1	-0.12	-0.07	0.99	0.08
	Stop 4 bed 2	-0.15	-0.13	1.03	0.09
	Stop 4 bed 3	-0.17	-0.25	1.16	0.12
	Stop 5	0.09	0.13	0.99	0.08
	Stop 6	0.32	0.32	0.60	0.03
	Stop 7	0.21	0.10	0.96	0.13
	Stop 8	-0.27	-0.25	0.89	0.06

Key	FDZ	Fault Damage Zone
	IQR	Inter-QuartileRange
	P	Pearson Correlation Coefficient

Supplement Section S.4

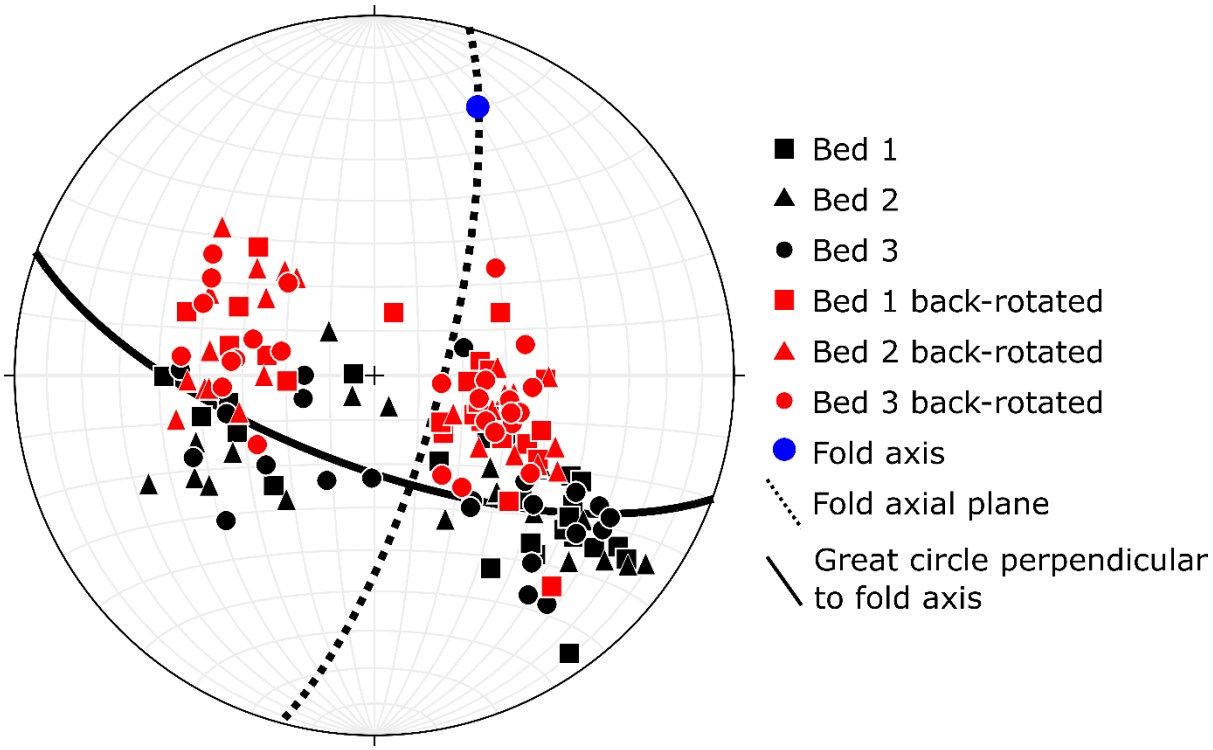

Figure S4.2. Schmidt net showing the orientations of deformation bands in three beds across a fold hinge. Deformation band present day orientation, and back-rotated orientations are shown. Present data orientation aligns with the great circle that is perpendicular to the fold axis indicating that deformation bands have been passively rotated with the folding of the host beds.

Supplement Section S.5

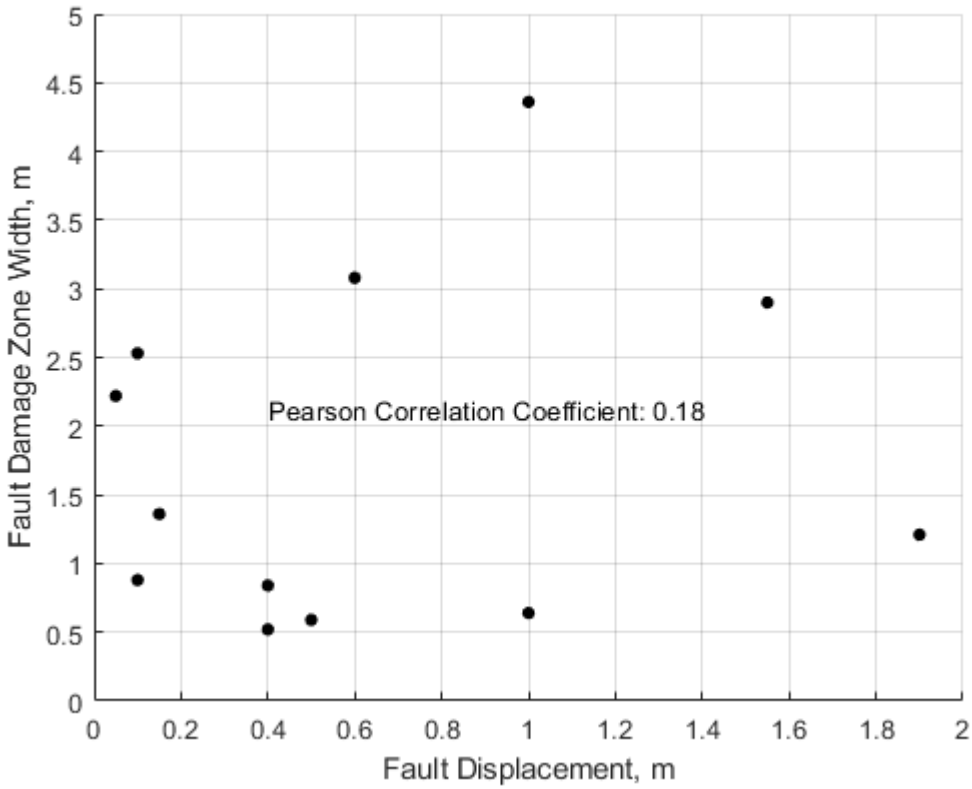

Figure S5.3. A plot to show the relationship between the fault displacement and the associated damage zone width. Fault displacement was measured where true displacement could be calculated from slip vector orientations and the separation of sedimentary markers across the fault plane (Shipton et al., 2006). Data shows that there is no correlation between the width of a damage zone and the offset of the associated fault.

Supplement Section S.6

Table S6.3. Table to show estimated permeability values. Equation used to estimate permeability from porosity: $\ln k = 21.41 + 11.425\ ln\phi_e + 1.327(ln\phi_e)^2$ (Wu, 2005). Order of magnitude reduction (OoMR) was calculated using: $OoMR = log_{10} \frac{Host\ Rock\ Permeability}{Deformation\ Band\ Permeability}$

	Porosity (%)	Permeability (mD)	Order of magnitude reduction
D2 Host Rock	13.00	38.00	1.98
D2 Deformation Band	5.00	0.40	
D3 FDZ Host Rock	20.00	645.00	1.45
D3 FDZ Deformation Band	12.00	23.00	
D3 non-FDZ Host Rock	19.00	449.00	1.95
D3 non-FDZ Deformation Band	9.00	5.00	

Supplement Section S.7

Table S7.4. Table to show the correlation statistics from porosity analysis of different band kinematics shown in Figure 9.

Porosity Analysis	Band Kinematics	Pearson	R^2
Host Rock and Deformation Band	*D2 CSB, D3 CSB, SECB*	0.69	0.47
	D2 CSB	0.72	0.51
	D3 CSB	0.06	0.00
	SECB	0.56	0.32
Host Rock and Absolute Porosity Reduction	*D2 CSB, D3 CSB, SECB*	0.55	0.30
	D2 CSB	0.79	0.62
	D3 CSB	0.97	0.94
	SECB	0.14	0.02

Supplement Section S.8

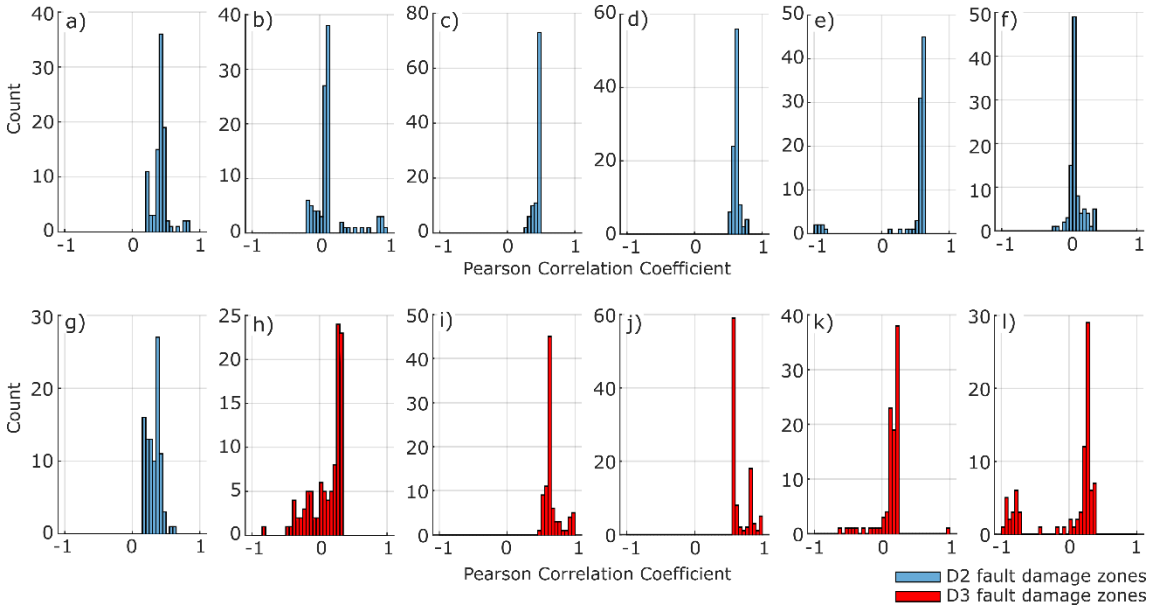

Figure S8.4. Histograms to show Pearson correlation coefficient values established from multiple scan-lines along deformation band maps from fault damage zones (FDZs). D2 FDZ and D3 FDZ are differentiated by colour. Many analyses have a main peak ca. 0.5 indicating a positive relationship between the spacing of deformation bands and the distance of those bands from a fault plane. However, within the dataset, there are peaks at values that are closer to 0. E.g.: in b) where the peak value is ca. 0.1 or h) where there is a cluster of peaks around 0. Peaks that have Pearson values that are close to zero indicate that there is no relationship between spacing and distance from the fault plane and is indicative of regular spacing. The range in Pearson values for each outcrop indicates that the spacing between deformation bands and the distance from a fault plane are not described by a simple relationship and that this relationship can vary on the outcrop scale.

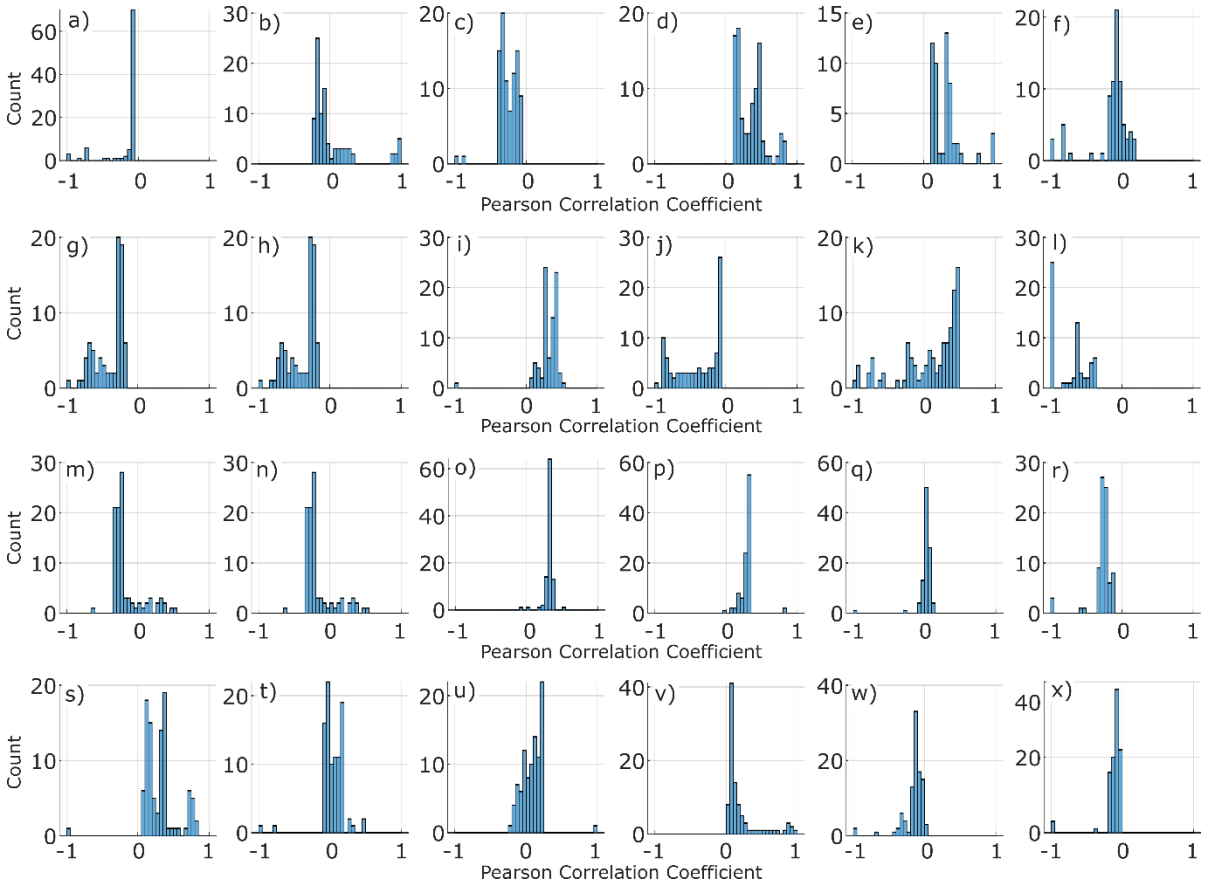

Figure S8.5. Histograms to show Pearson correlation coefficient values for D3 deformation bands that are characterised by minimal offset and a regular spacing (D3 non-FDZ). The spacing of bands has been compared to the distance perpendicular to strike. Most histograms show a peak ca. 0. This indicates no relationship between spacing and distance. There are, however, instances of a large spread of Pearson data e.g. in image (k). 12 out of 28 outcrops analysed have a spread of Pearson data that is greater than 1. This indicates that there can be scan-lines across a single outcrop that are identifying band populations with positive, negative, and zero correlation between the spacing and distance from the image origin.

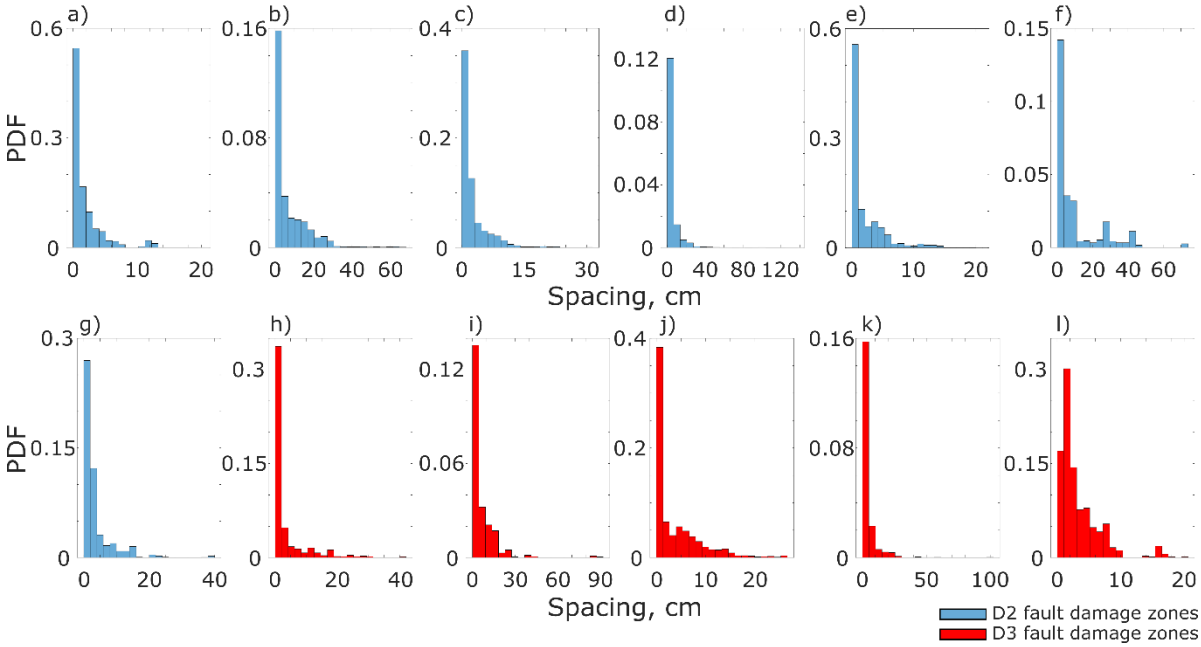

Figure S8.6. Histograms to show the frequency distribution of absolute spacing measurements between bands in fault damage zones. The probability density function is on the y-axis. The histograms have a positive skew representing the decay of damage away from the fault plane.

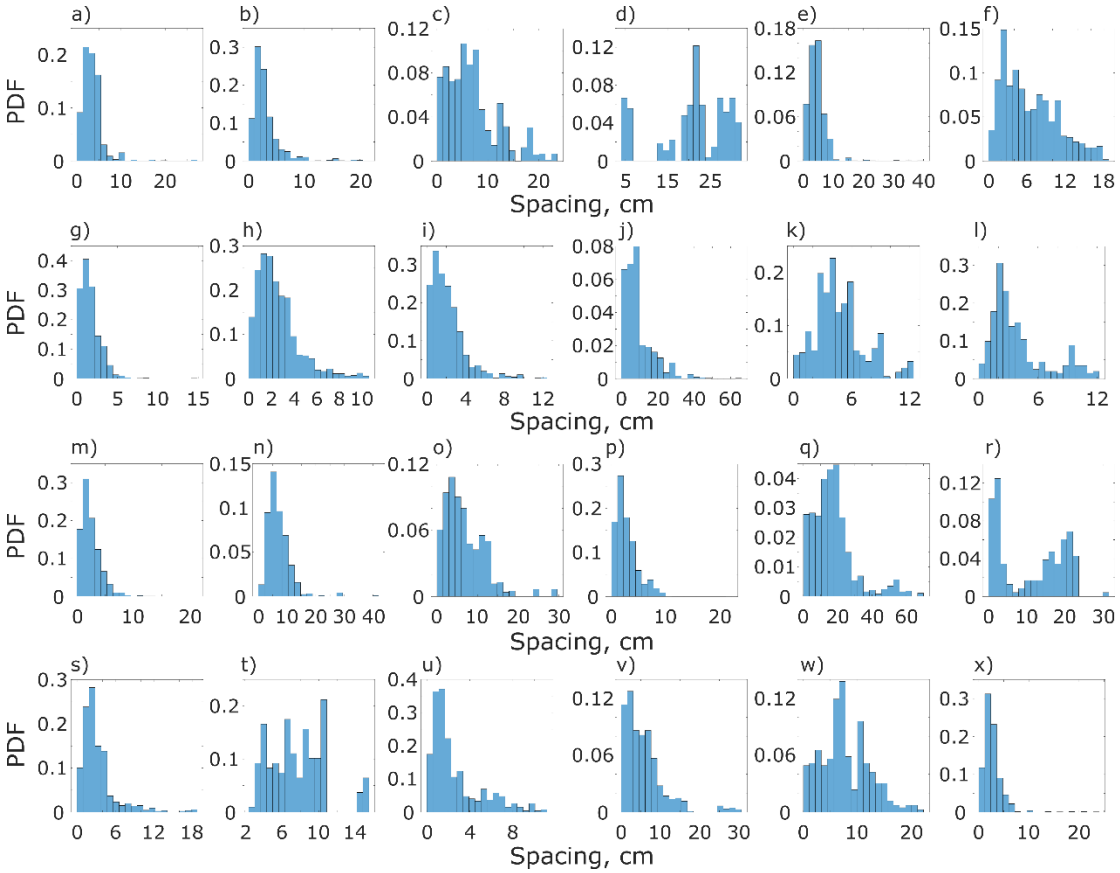

Figure S8.7. Histograms to show the probability density function of spacing of D3 deformation bands observed in outcrops that are not directly adjacent to a fault. In these outcrops, deformation bands show a 'regular' spacing. The bands analysed in this plot are characterised by minimal offset / no observable offset. Histogram plots are not consistent. Some have a bimodal distribution (e.g. d and l). Some are characterised by a normal distribution (e.g. k and t). Many have a positive skew yet compared to 'fault-associated' band spacing, there is a broader spread, indicative of regular spaced bands, with noise (Fig. 10).

References

Allmendinger, R. W., Cardozo, N., and Fisher, D. M.: Structural geology algorithms: Vectors and tensors, Cambridge University Press, 2011.
Shipton, Z. K., Soden, A. M., Kirkpatrick, J. D., Bright, A. M., and Lunn, R. J.: How thick is a fault? Fault displacement-thickness scaling revisited, 2006. 2006.
Wu, T.: Permeability prediction and drainage capillary pressure simulation in sandstone reservoirs, 2005. Texas A&M University, 2005.